energies

MDPI

Article

Study of Combustion Process Parameters in a Diesel Engine Powered by Biodiesel from Waste of Animal Origin

Piotr Łagowski [1,*], Grzegorz Wcisło [2] and Dariusz Kurczyński [1]

[1] Department of Automotive Vehicles and Transportation, Faculty of Mechatronics and Mechanical Engineering, Kielce University of Technology, Al. Tysiąclecia Państwa Polskiego 7, 25-314 Kielce, Poland; kdarek@tu.kielce.pl

[2] Department of Bioprocess Engineering, Energy and Automation, Faculty of Production Engineering and Power Technologies, University of Agriculture in Krakow, ul. Balicka 116, 30-149 Krakow, Poland; grzegorz.wcislo@ur.krakow.pl

* Correspondence: p.lagowski@tu.kielce.pl; Tel.: +48-41-3424332

Abstract: The use of biofuels is one way to reduce the increasingly visible harmful effects of diesel engines on the environment. At the same time, it is also a way to gradually reduce dependence on depleting oil resources. New sources for biodiesel production are currently being sought out. The authors of this article have produced esters from animal fat waste, obtaining a biofuel that can power diesel engines while obtaining a way to manage unnecessary waste. For this to be possible, it is necessary to confirm the possibility of using such biofuel to power compression ignition engines. To this end, it is moribund to conduct experimental tests on an engine dynamometer. The results of such studies made it possible to determine how such esters affect the parameters of the combustion process, which was the goal of the authors of this paper. In order to determine the effect of this biofuel on the parameters of the combustion process, indicator graphs of the pressure course in the engine cylinder were recorded. On their basis, heat release characteristics were drawn up and their most important indicators were determined. In addition, the parameters of the indicator charts were determined, such as the maximum pressure and the degree of its build-up during the combustion process. These tests were carried out on a Perkins 1104D-E44TA compression ignition engine, which is widely used in the construction industry as well as in agriculture. In order to be able to compare these results with diesel fuel, the same tests, under the same conditions, were carried out while feeding the engine with diesel fuel. It is worth noting that the tested esters were produced using a reactor designed and built by one of the co-authors of this publication. This reactor is used for the non-industrial production of biofuels from oils of various origins. Studies have shown that feeding the engine with esters results in an increase in the maximum fuel consumption of about 15%. This is dependent on the load and speed. Indicator graphs and their analysis indicated that feeding the engine with esters at lower loads results in higher maximum combustion pressures, depending on the engine load, compared to diesel fuel values by a maximum of about 10%. The calculated values of the degree of pressure increase during the combustion process showed that feeding the engine with esters at most loads results in an increase of up to 40% maximum. This is especially the case for a speed of 2200 rpm. In the case of parameters related to heat release characteristics, the relationship is the opposite, and feeding the engine with esters compared to diesel fuel results in higher maximum amounts and rates of heat release. These values are higher for esters from 20 to 40%. In addition, the percentage burnout of the fuel dose confirmed the information found in other publications that feeding the engine with biofuels causes faster combustion compared to diesel.

Keywords: biodiesel; animal fat esters; combustion process; heat release characteristics

Citation: Łagowski, P.; Wcisło, G.; Kurczyński, D. Study of Combustion Process Parameters in a Diesel Engine Powered by Biodiesel from Waste of Animal Origin. *Energies* **2024**, *17*, 5857. https://doi.org/10.3390/en17235857

Academic Editors: Hubert Kuszewski and Paweł Woś

Received: 14 October 2024
Revised: 14 November 2024
Accepted: 19 November 2024
Published: 22 November 2024

1. Introduction

Despite the intensive development of electric vehicles and drives, compression ignition engines are still widely used where high torque values and continuous uninterrupted operation are required. Examples include vehicles used in road transport and heavy vehicles used in road construction, but also vehicles used in agriculture [1–5]. Despite the wide range of advantages of this type of engines, the main problem faced by designers is their negative impact on the environment, in particular with emissions of nitrogen oxides, but also in terms of significant emissions of particulate matter, whose elimination significantly complicates exhaust gas after-treatment systems [6–8]. An important factor determining the impact of these engines on environmental pollution is the type of fuel used and its injection, which directly affects the quality of the combustion process. Trying to find alternatives to diesel fuel that can be widely used to power diesel engines should take into account the ability of these fuels to not only self-ignite but also to form a fuel–air mixture. These parameters directly affect, for example, the auto-ignition delay period, and thus the course of the combustion process and emissions of environmentally harmful components of the exhaust gas [9,10]. Among the most important processes that occur in compression ignition piston internal combustion engines is the combustion process. One of the ways that allow for its wide-ranging evaluation is the indicator diagram, which is the course of pressure in the cylinder during the combustion process. This chart is the final result of primarily thermodynamic processes that occur during combustion. Using the indicator graph, it is possible to determine the heat release characteristics during the combustion process, which makes it possible to determine and evaluate the contribution of kinetic and diffusive combustion or the maximum amount and rate of heat release [11–15]. Among the important factors that significantly affect the combustion process and heat release characteristics is the type and quality of injected fuel with which the engine is powered. Currently, biofuels are widely used to power compression ignition engines in addition to diesel fuel. Their use allows for a significant reduction in harmful components in the exhaust gas [16,17]. From the definition that operates in the literature [10,18–21], biofuels are called fuels, which can be in liquid form or in gaseous form obtained from biomass. We can divide these biofuels into four generations. The different generations depend on the raw material from which the oil is produced, from which esters are then obtained. In the case of the first generation of biofuels, the basic raw material from which they are produced are oils and esters obtained from food crops [11,22,23]. The second generation of biofuels is primarily non-food crops and produced from agro-food industry waste, which we can include, among other things, waste from the tanning industry [2,24–31]. Another generation is biofuels, which are derived from organic matter, which is obtained from the raw materials of crops modified by molecular biology techniques. These include algae [32,33]. The fourth generation of biofuels are the fuels of the future, and their development is aimed at closing the carbon balance and eliminating its negative impact on the environment. The current literature contains many publications on biofuels obtained from various materials, the amount of which is constantly increasing as a result of the progress of civilization. This progress produces various types of waste that are primarily the result of human activity. One way to manage these wastes is to produce biofuels from them. These wastes are primarily waste from organic matter. These biofuels, according to the previously described classification, are classified as second-generation biofuels. Organic waste of this kind also includes animal waste. The extraction of biofuels from them is much less developed than those produced from plants. Its significant advantages include the low cost resulting from processing not a raw material such as food but a waste that must be disposed of, which is associated with high costs. In the literature [34], the raw material from which the authors obtained biodiesel was waste chicken and pork fat, the properties of which complied with the requirements of the relevant standards. On the other hand, the authors of paper [35] obtained biofuel from corn oil and chicken fat. On the other hand, the authors of paper [36] note the small number of publications related to the study of engines fueled by biofuels from animal waste, especially the lack of studies related to the course of the combustion process in engines fueled by these biofuels.

In paper [37], the authors studied three types of HVO and RME fuels, as well as DF, which was the base fuel and to which they compared the results from the two earlier fuels. The authors in that work showed that hydrotreated vegetable oil and RME canola oil esters burned more slowly compared to diesel fuel. A similar fuel was tested by the authors of paper [38], which was hydrotreated vegetable oil HVO compared to diesel fuel. The authors of that work showed that the combustion process in an engine fueled with hydrotreated vegetable oil starts earlier than when fueled with DF, which is due to the higher cetane number.

In turn, the authors of publication [39] presented the results of a wide range of studies of the combustion process as well as emissions of an engine fueled with biofuel obtained from fish industry waste. In addition, three blends of biofuel from fish oil with standard diesel fuel were tested. As the authors of the paper found, the highest p_{max} values were obtained by powering the engine with biofuel from waste fish oil. In addition, this fuel burns faster than DF. The results showed a favorable effect of using blends of this biodiesel with diesel fuel on the stability of maximum combustion pressure values. The analysis of the results of the study showed that waste fish oil fuel has higher thermal efficiency and lower heat loss during the combustion process compared to diesel fuel. In another publication, the authors [26] describe the significant advantages of biofuel from waste fat. According to the authors, these fuels have significant amounts of saturated fatty acids, significantly increasing the cetane number of these fuels. As studies [40] show, a high cetane number value causes combustion to occur at lower temperatures. This is important and allows for lower concentrations of nitrogen oxides in the exhaust gas. On the other hand, the authors of the paper by Varuvel et al. [41] presented the results of tests on biofuel obtained from waste fish fat and its blends with diesel fuel. The study showed an increase of about 2% BTE for pure biodiesel. The research showed at the same time that the time of auto-ignition delay was shortened and the speed of the combustion process was increased. In addition, higher combustion pressures were obtained for blends of this biofuel with diesel fuel than for diesel fuel alone. In publication [42], the authors conducted a study of biofuel obtained from waste animal fat. Blends of this biofuel with diesel and bioethanol were also studied. The study showed an increase in specific fuel consumption (BSFC) when the engine was fueled with biofuel compared to diesel, while higher BSFC was obtained for blends containing 20% bioethanol compared to diesel. Analyzing the effect of the biofuel on the combustion process, the authors indicated that the maximum combustion pressure in the cylinder when the engine was fueled with biodiesel was about 1.2% higher compared to diesel. In addition, it was noted that the combustion process of this biofuel started at earlier crankshaft rotation angles compared to diesel, having an apparent effect on the auto-ignition delay period, which is also confirmed by the research presented in this article and publication [43]. An increase in the addition of bioethanol to the fuel mixture resulted in an increase in auto-ignition delay and thus a later onset of combustion.

In [44], the authors studied biofuel from waste animal fats and their blends enriched with metal oxide nanoparticles. In that study, blends of biodiesel and diesel fuel with zinc oxide nanoparticle additives resulted in increased engine efficiency and reduced exhaust emissions. The transesterification process yielded SF biodiesel, and zinc oxide nanoparticles were added as additives to improve the combustion process. Sheep fat (SF) biodiesel of 20% by volume was blended with conventional DF diesel of 80% (B20). Higher in-cylinder combustion pressures and BTE were obtained with B20 + ZnO 100 ppm and B20 + ZnO 50 ppm blends. In contrast, BSFC showed a decrease compared to fuel blends without nanoparticles, but at a higher load.

The authors of paper [45] evaluated the performance of a diesel engine powered by blends of biodiesel and diesel fuel from waste chicken fat. In the study, blends of biodiesel from chicken oil with diesel fuel were prepared. They were then tested on the engine for exegetical and exo-economic evaluation. As the study showed, feeding the engine with biofuel resulted in a deterioration of exegetical and exo-economic efficiency, but, nevertheless, there is a kind of way to develop waste products into an energy source.

Most often, scientists obtain esters from new raw materials under laboratory conditions, while the authors of this paper produced esters from the waste of an animal skin processing plant. These esters were produced using a reactor built and patented by Grzegorz Wcisło, one of the co-authors of this paper (Polish Patent Office, patent number 218554). The esters are abbreviated AMEs in the paper, while the diesel fuel is designated DF. The esters in their pure form, without any additives, were used to power a Perkins 1104D-E44TA (Perkins Engines Company Limited, Frank Perkins Way, Eastfield, Peterborough, PE1 5NA, UK) compression ignition engine. The authors of this publication conducted experimental tests to determine how feeding the engine with these esters would affect its performance parameters including the combustion process.

2. Experimental Work

In compression ignition piston internal combustion engines, the working medium is compressed air into which fuel is injected at the end of the compression stroke. As a result of high pressure and temperature, the vaporized and mixed fuel and air undergo self-ignition and combustion. The course of the combustion process is strongly dependent on the type and quality of the fuel being burned as well as the parameters of the fuel injection process itself.

As a result of combustion, heat is released, causing a change in the pressure and temperature of the working medium in the cylinder. The heat released causes a change in the cylinder pressure, which, presented as a function of engine crankshaft rotation, is called an indicator diagram. It is the final result of the thermodynamic, thermochemical, and hydro-aerodynamic processes and heat transfer occurring in the cylinder of a reciprocating internal combustion engine [46–49]. In addition, it is also the primary quantitative and qualitative source of information about these processes and indices of engine operation. The parameters of the indicator diagram depend on the course of the combustible mixture formation process, which is influenced by fuel injection and parameters related to the supply of oxidizer to the cylinder. The aforementioned quantities have a significant influence on the parameters of the combustible mixture and exhaust emissions [50,51].

A system from AVL was used to record indicator graphs during the implementation of the study. On the basis of the indicator graphs, using the software of the same company [52], graphs of the amount of heat release during the combustion process were made, and their maximum values, denoted in the paper by HR_{max}, were determined. In addition, the maximum rate of heat release during combustion, denoted HRR_{max}, was determined. The maximum combustion pressures p_{max} and the maximum pressure build-up increments $dp/d\alpha_{max}$ were determined. The above-mentioned parameters obtained when the engine was fed with AME esters were compared with those obtained under the same operating conditions of the engine, but fed with DF, which met the requirements of the PN-EN590+A1 standard [53].

Experimental tests were carried out on a dynamometer bench located at the Thermal Engine Laboratory of the Swietokrzyska University of Technology. Two load characteristics were chosen as engine operating conditions: one at the speed of maximum torque, i.e., 1400 rpm, and the other at the speed of maximum engine power, i.e., 2200 rpm. The lowest engine load was a torque value of 20 Nm, and the next point was 50 Nm. Then, the next load points were obtained by increasing the torque by 50 Nm until the maximum torque was reached. Both fuels were tested under the same operating conditions, which allowed them to be compared.

2.1. Description of the Engine and Test Stand

The Perkitns 1104D-44TA diesel engine used in this study is used to power off-road machinery, including agriculture and the construction industry. This engine meets STAGE IIIA emission standards as well as another EPA Tier 3-type standard. It is a modern engine equipped with a direct injection power system with a rotary injection pump from Delphi and an eight-valve valve train with gear transmission to the camshaft. In addition, the engine is equipped with turbocharging and a charge air cooler. The most important technical data of the engine used in this study are provided in Table 1.

Table 1. Engine data and specifications Perkins 1104D-44TA.

Parameter	Value
Manufacturer	Perkins
Cylinder arrangement	Row
Number of cylinders	4
Displacement capacity	4.4–10^{-3} m^3
Compression ratio	18.2:1
Type of power system	Direct
Injection pump model	Delphi DP310 rotary pump
Air supply system	Turbocharger
Camshaft placement	In the engine block
Camshaft drive	Sprockets
Number of valves per cylinder	2
Maximum engine power	75 kW
Maximum torque	416.0 Nm
Maximum n power speed	2200 rpm
Maximum torque speed	1400 rpm

The test stand used in the experiments is equipped with an eddy current brake AMX-200/6000 from Automex (ODIUT Automex, Gdańsk, Poland) with an absorption power of 200 kW and a maximum torque of 700 Nm. Fuel consumption was measured using a strain gauge from the same company as the brake. The block diagram of the stand is shown in Figure 1.

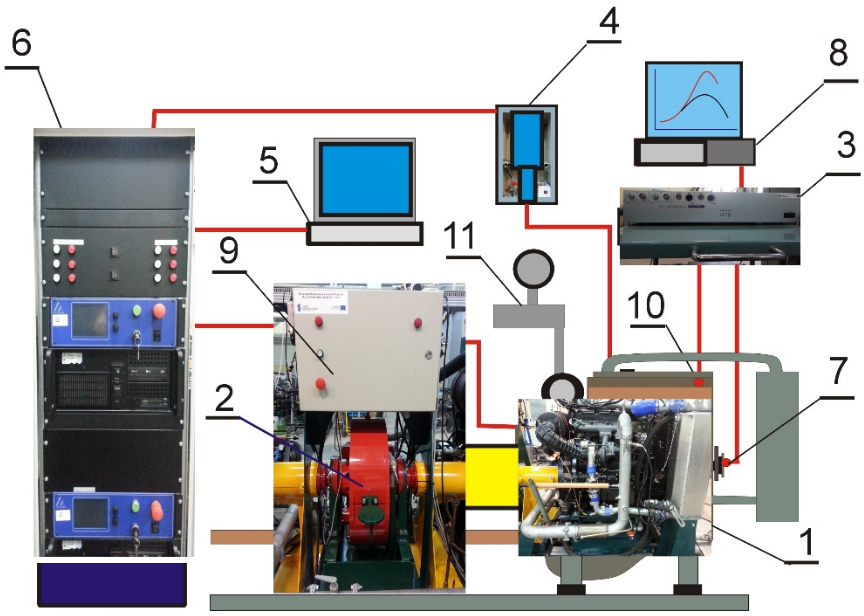

Figure 1. Construction of the test stand, where 1—Perkins 1104D-44TA engine; 2—Automex electrorotor brake; 3—AVL Indicom 612 engine cylinder pressure indexing system; 4—ATMX2040 strain gauge mass fuel consumption meter; 5—computer; 6—measurement cabinet with control system; 7—marker from AVL for measuring the engine crankshaft rotation angle; 8—system management computer for measuring and recording fast variable quantities; 9—brake measuring module; 10—piezo-quartz cylinder pressure sensor from AVL; 11—mass air flow meter.

The test stand where the tests were carried out is equipped with an AMX-200/6000 eddy current brake from Automex with an absorption power of 200 kW and a maximum torque of 700 Nm. Fuel consumption was measured using a strain gauge from the same company as the brake. The block diagram of the test stand on which the tests were carried out is shown in Figure 2.

Figure 2. Photo of the GW200 reactor used for ester production (Malopolskie Center of Renewable Energy Sources "BioEnergia", Krakow, Poland).

For the measurement of fast-variable quantities such as the course of pressure in the engine cylinder as a function of the angle of rotation of the crankshaft, systems specially configured for this purpose are most often used [54]. On the bench, the measurement system from AVL IndiSmart 612 (AVL List GmbH, Graz, Austria) was used for this purpose. AVL's GH13P/AG04 (AVL List GmbH, Graz, Austria) piezoelectric sensor was used to measure the pressure in the cylinder. It was placed in place of the glow plug. Measurements of the above-mentioned cylinder pressure were recorded as a function of crankshaft rotation measured with an AVL 365C encoder (AVL List GmbH, Graz, Austria) with a resolution of $\Delta\alpha = 0.5°$ CA. The entire system for recording the fast-variable quantities was managed using AVL Indicom Mobile 2012 software. Table 2 shows the apparatus used for indexing engine cylinder pressure. The bench was also equipped with an apparatus for measuring emissions of the primary components of the exhaust gas Horiba Mexa-1600DEGR (Horiba, Ltd., Kyoto, Japan) and particulate matter Horiba Mexa-1230PM (Horiba, Ltd., Kyoto, Japan), the results of which are presented in another publication [55].

Table 2. Specification of apparatus for measuring high-speed quantities.

Destination	Type/Manufacturer
Cylinder pressure	AVL GH13P/AG04 (AVL List GmbH, Graz, Austria)
Crankshaft rotation angle	AVL 365 C (AVL List GmbH, Graz, Austria)
Data processing	AVL IndiSmart 612 (AVL List GmbH, Graz, Austria)
Software	AVL IndiMobile 2012 (AVL List GmbH, Graz, Austria)
Load brake	AMX200/6000 (ODIUT Automex, Gdańsk, Poland)

2.2. Fuels Tested

Compression ignition engines require fuels with good combustible mixture formation properties. These properties can include appropriate chemical composition, formation of the smallest possible droplets of injected fuel, and evaporation [56,57]. Important parameters that affect the combustion process of the fuel can also include the cetane number, which determines its self-ignition ability. This parameter affects the auto-ignition time and thus the course and efficiency of the combustion process. The ever-increasing requirements to reduce diesel fuel consumption are causing a search for new fuels to power compression ignition engines. These include alternative fuels produced from vegetable oils or gaseous fuels, etc. Fuels belonging to this group are also esters derived from animal fats. Such fuel was used in the study. The material from which the esters were produced was waste from the animal skin processing industry, which is used on a large scale in the clothing and footwear industries. Such waste, if not used in industry, requires difficult and expensive disposal. The authors of this publication, using methyl alcohol and an alkaline catalyst, have produced animal-derived methyl esters from such waste. The basic physical and chemical properties of this fuel and diesel are shown in Table 3.

Table 3. Physical and chemical properties of diesel fuel and produced esters from animal waste.

Property	Method	Value	
		AME	DF
Higher heating value, MJ/kg	PN-C-04375-3 [58]	42.23	46.32
Lower heating value, MJ/kg	PN-C-04375-3 [58]	38.67	43.34
Flash point, °C	EN ISO 2719 A [59]	116.2	58.5
Viscosity at 40 °C, mm^2/s	EN ISO 3104 [60]	4.32	2.11
Density at 15 °C, g/cm^3	PN-EN ISO 12185 [61]	0.883	0.828
Cetane number (CN)	EN ISO 5165 [62]	55.4	51.7
Water content, mg/kg	EN ISO 12937 [63]	84	24
Cold filter plugging point, °C	EN 116 [64]	13	−27
Lubricity (WSD), µm	PN-EN ISO 12156 (1) [65]	614	408
HPLC total aromatics, % (m/m)	Infrared analysis (instrument TD PPA-PetroSpec by PAC)	-	16.3
HPLC PNA aromatics, % (m/m)	Infrared analysis (instrument TD PPA-PetroSpec by PAC)	-	1.4
FAME content, % (*v*/*v*)	(DF-Irox Diesel apparatus, PN-EN 14103 [66])	100	0.1

Compared to DF, AMEs produced from animal waste have a higher cetane number and higher viscosity, density, and ignition temperatures. AMEs have a lower calorific value compared to DF. In addition, disadvantages include their higher water content and inferior low-temperature properties, which significantly hinder their normal use in engines, making it necessary to modify them, for example, by using heaters, etc. The implementation of this study did not check the effect of this fuel on the durability of the power system or crank–piston components. During the execution of the tests, in order to ensure the proper conduct of the tests, the esters were placed in a special tank, which allowed us to maintain their temperature at a constant level of about 40 °C. During the tests, there were no problems related to the operation of the supply system and the engine itself. The tests were carried out on the same feed system, i.e., the injection pump, injectors, and filters, as the tests when feeding the DF engine. In doing so, it should be remembered that esters of higher fatty acids, when added to diesel fuels, quickly undergo an oxidation process. The oxidation process causes the formation of various types of deposits that can lead to the clogging of fuel filters and the degradation of fuel system components such as fuel lines and seals [67]. For this study, esters without additives were used to improve their physical and chemical properties, including low-temperature properties. The tested esters were produced using a reactor patented and built by one of the co-authors of this paper [68]. This reactor with one cycle of operation, which takes about 1.5 h, allows 50 L of esters to be produced. The production of esters in the reactor can be carried out in a one-stage or two-stage process at temperatures of 60/120 °C. The principle of the reactor itself is to use oil or methyl or ethyl alcohol for transesterification in the presence of a suitable catalyst. During the production of AME esters, the authors used methyl alcohol, while potassium hydroxide KOH was used as an alkali catalyst. A photo of the reactor in the laboratory is shown in Figure 2.

3. Test Results and Analysis

As previously mentioned, tests were realized for two load characteristics at constant speeds of 1400 and 2200 rpm. During the tests, the engine was fed with AME esters and DF for comparison. During the tests, the basic parameters of the engine's operation were recorded, paying particular attention to indicators relating to the combustion process. The results of these measurements were corrected to normal conditions to ensure their comparability. Similar to the work of [69], cylinder pressure waveforms were recorded where, in order to ensure the repeatability of test conditions, graphs averaged over consecutive 200 duty cycles were used to analyze and produce heat release characteristics. From these charts, the maximum values p_{max} and the crankshaft rotation angles at which they occurred α_{pmax} were determined. These data made it possible to determine the effect of the tested fuels on the degree of pressure buildup in the cylinder $(dp/d\alpha)_{max}$.

In order to increase the accuracy of the measurements, all measurements were recorded in files for successive fixed measurement conditions. Once the engine operating conditions were stable at each measurement point, the measurements were recorded for about 120 s. As in other works [70] that provide statistical analyses for the recorded measurement data, the standard uncertainty of the arithmetic mean of the measurement was calculated. The tests showed a significant decrease in torque when feeding the engine with AMEs compared to the parameters obtained for DF. For a speed of 1400 rpm, the decrease in maximum torque is 40 Nm. For a speed of 2200 rpm, it is 50 Nm, to the disadvantage of AMEs. The decrease in these parameters is related to the significantly higher viscosity of AMEs compared to DF, and thus it affects the formation and combustion of the combustible mixture. These results are consistent with studies presented in the work of [71,72]. This may create difficulties for the use of this biofuel in heavy-duty engines. During the implementation of this study, the content of basic components in the exhaust gas and particulate emissions were also measured. The results of these tests are presented in another publication by the authors [55]. The engine load conditions were presented in a similar form to the publications [54,69], where the engine load was converted to brake mean effective pressure (BMEP). During the tests, measurements of exhaust and particulate emissions were also recorded. The results of these studies are presented in [55]. Engine load conditions during this study along with fuel consumption per duty cycle are shown in Table 4.

Table 4. Experimental engine load conditions and fuel consumption when operating the engine according to load characteristics of 1400 and 2200 rpm.

T Load (Nm)	Load (%)	BMEP (MPa)	Fuel Mass Per Cycle (mg/cycle) 1400 rpm		2200 rpm	
			DF	AME	DF	AME
20	4.55	0.06	11	12	14	16
50	11.36	0.14	15	17	18	19
100	22.73	0.29	23	26	26	29
150	34.09	0.43	32	34	35	40
200	45.45	0.57	39	45	45	52
250	56.82	0.71	53	53	51	68
300	68.18	0.86	57	62	61	70
350	79.55	1.00	65	72	67	-
400	90.91	1.14	71	81	-	-
440	100	1.26	82	-	-	-

As can be seen from Table 4, feeding the engine with AME esters, depending on the load, increases fuel consumption by a maximum of 15% compared to DF. Figures 3 and 4 show pressure profiles recorded when the motor is operated according to load characteristics of 1400 and 2200 rpm for example loads.

A comparison of the maximum pressures during the combustion process for the fuels we studied is given in Figure 5, while Figure 6 shows the values of the angles at which they occurred. For AME fuel in the range of average loads between 50 and 150 Nm and from 350 to 400 Nm, a higher p_{max} was obtained compared to DF by about 10%. These results are consistent with the authors' data presented in the literature [42]. With the characteristics of 2200 rpm at low loads, the relationship is similar; for T = 50 and 100 Nm, the highest values of p_{max} were obtained for AME fuel. For the smallest load at T = 20 and 150 Nm for AME fuel, slightly smaller p_{max} values were obtained compared to DF by about 2%. Considering higher loads, values of maximum pressures are similar for both tested fuels.

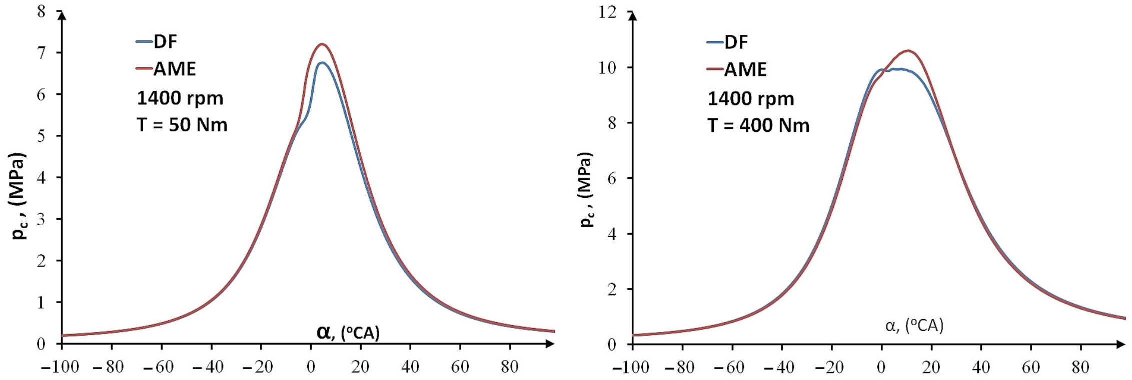

Figure 3. Example pressure profiles recorded for load characteristics at 1400 rpm.

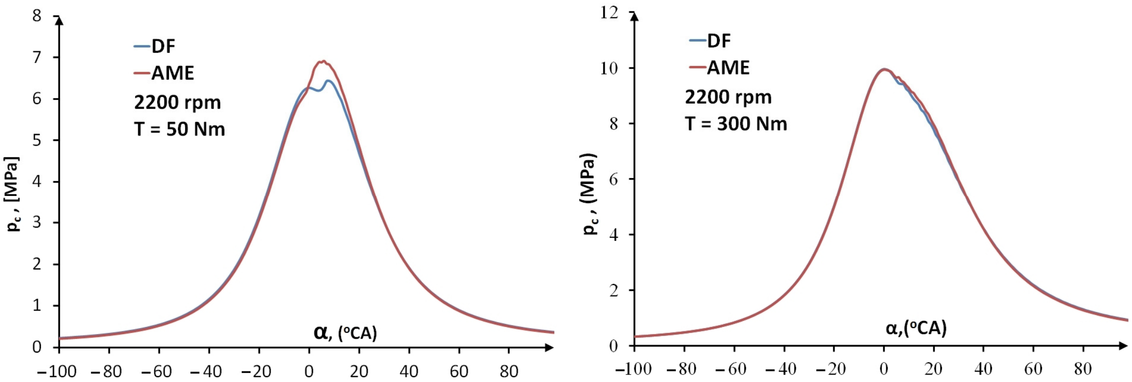

Figure 4. Example pressure profiles recorded for load characteristics at 2200 rpm.

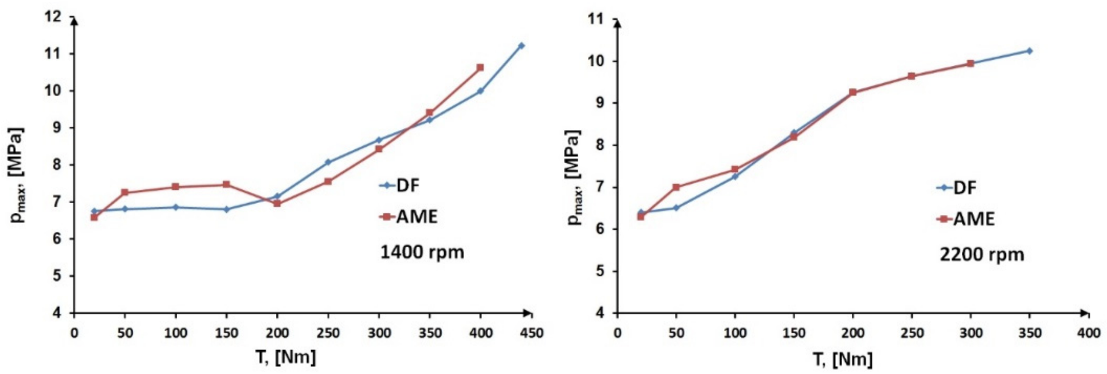

Figure 5. Graphs of maximum combustion pressures p_{max}.

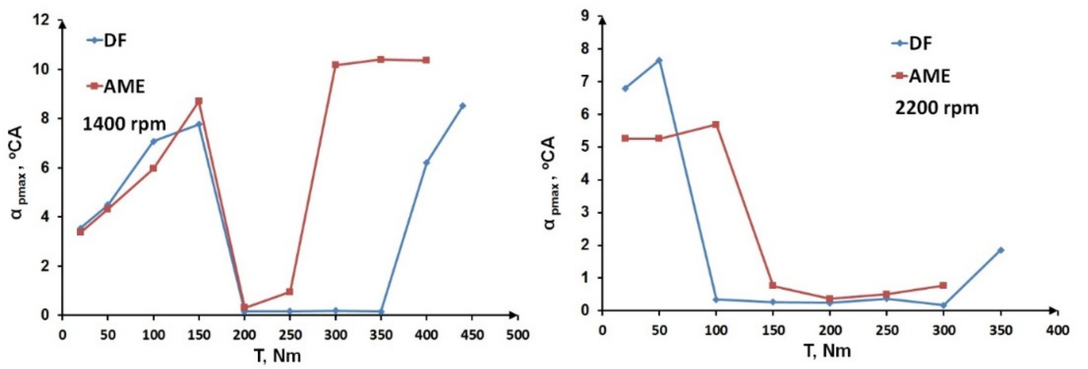

Figure 6. Graphs values of the rotation angles of the crankshaft for which maximum pressures p_{max} occurred.

When feeding the engine AMEs for 1400 rpm and for torques ranging from 20 to 100 Nm, p_{max} occurred slightly earlier than for DF. For further torques from 150 Nm to 400 Nm, p_{max} occurred later when feeding AMEs compared to DF, especially for loads from 300 to 400 Nm, where the difference is about 10° CA at most.

Analyzing the results for 2200 rpm, the relationships are similar to those for 1400 rpm, but the differences in α_{pmax} values are greater at lower loads. For loads from 20 to 50 Nm when feeding the AME engine, the maximum combustion pressure occurred earlier compared to DF by about 2° CA. For other loads, the relationship is reversed.

The results with plots of maximum pressure increments during the combustion process $(dp/d\alpha)_{max}$ are shown in Figure 7.

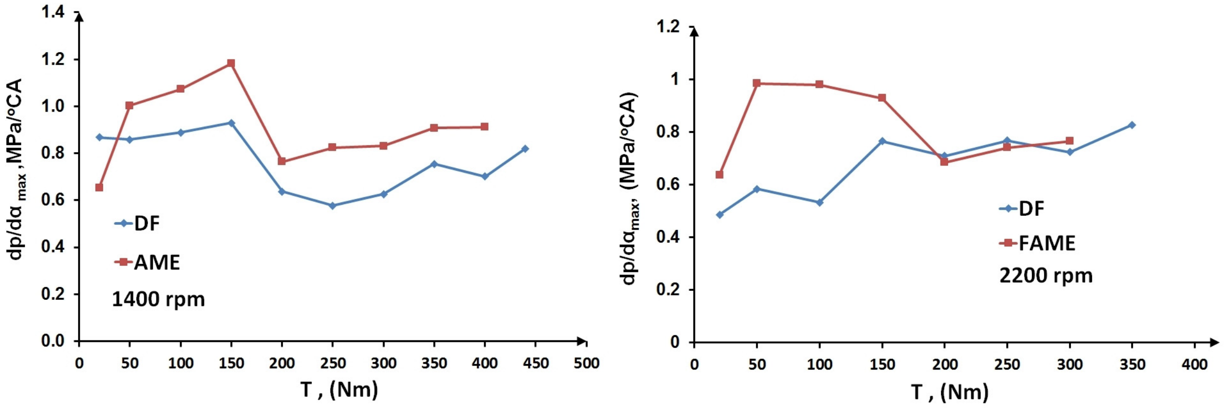

Figure 7. Maximum increments of cylinder pressure $(dp/d\alpha)_{max}$.

For the 1400 rpm characteristic, feeding the engine with AMEs compared to DF results in about 40% greater maximum combustion pressure increments compared to DF. Only for the lowest load of 20 Nm did the larger $(dp/d\alpha)_{max}$ occur for DF.

At 2200 rpm, the dependencies are similar. For loads from 20 Nm to 150 Nm and 300 Nm, the largest $(dp/d\alpha)_{max}$ occurred for AMEs, and they are much larger than for DF. Similar growth relationships of $(dp/d\alpha)_{max}$ for biofuels are described by the authors in article [56]. This is due to the higher oxygen content of this fuel and the higher cetane number, which shortens the auto-ignition delay period, causing the pressure to increase during the combustion process. For other loads, the values of $(dp/d\alpha)_{max}$ for both fuels are similar. The higher degree of pressure buildup for AMEs may have a significant impact on the durability of crank–piston components, and confirmation of this would require long-term durability tests feeding the engine with such fuel.

Characteristics of the amount and rate of heat release during the combustion process were prepared based on the averaged cylinder pressure from two hundred runs. Based on them, their maximum values were determined. Examples of the characteristics of the amount of heat release are included in Figure 8, while Figure 9 shows their maximum values. Powering an AME engine results in lower maximum heat release quantities HR_{max} compared to DF. These differences range from 1 to a maximum of 19% at the lowest engine loads. The lower amounts of heat release for AME are due to the lower heating value of this fuel compared to DF.

Figure 10 shows examples of HRR (heat release rate) characteristics, and Figure 11 shows their maximums.

The values of the maximum heat release rate HRR_{max}, in addition to the type of fuel used to power the engine, are dependent on engine load. For the characteristics of 1400 rpm as well as 2200 rpm, feeding the engine with AME fuel results in lower values of the heat release rate; this is particularly pronounced at low and medium engine loads in the range from 20 to 200–250 Nm. These values are higher for DF compared to AMEs by a maximum of about 44%, with larger differences at 1400 rpm. Only for the load characteristics prepared at 1400 rpm and loads from 300 to 440 Nm, HRR_{max} was slightly higher when the engine was fed with AME fuel compared to DF by about 7%. Similar correlations regarding the effect of feeding the engine with esters on HRR_{max} are confirmed by other studies [56,57]. This is due to the lower calorific value of esters and their higher density and viscosity, which adversely affects the formation and combustion of the combustible mixture.

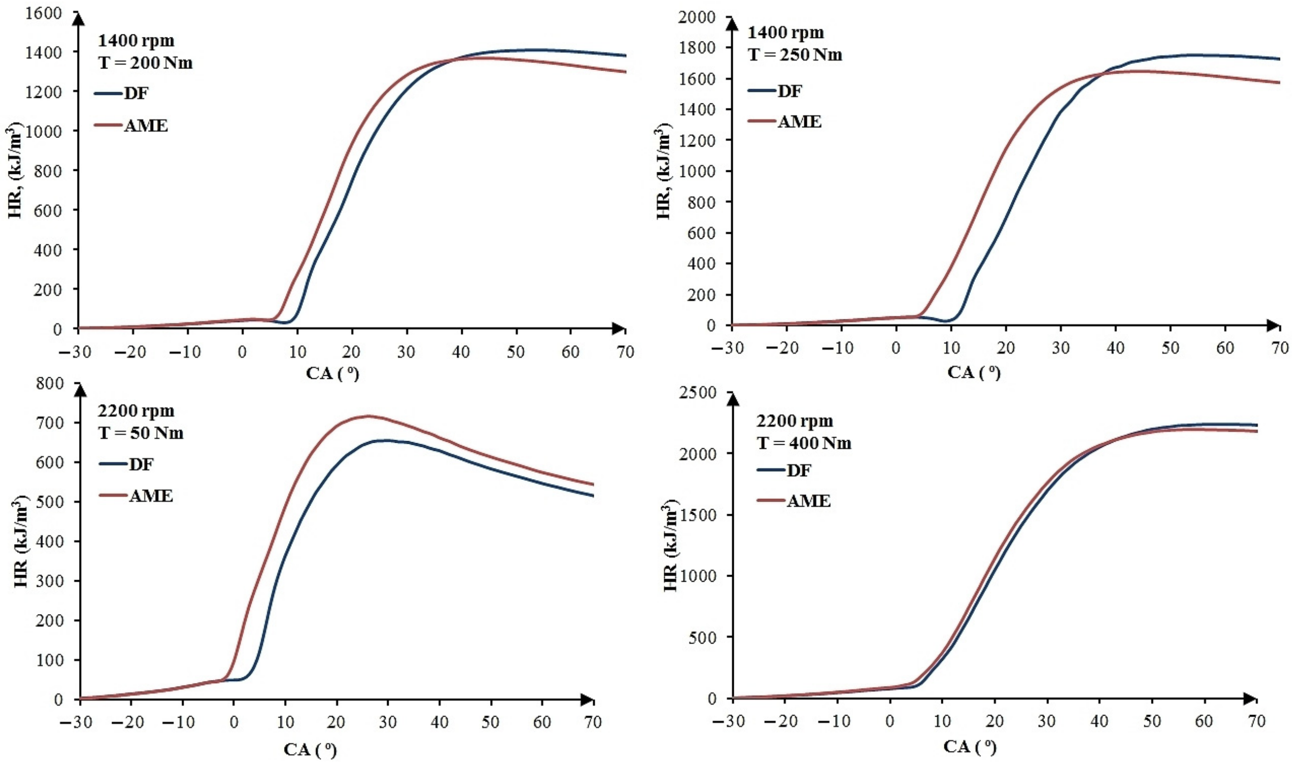

Figure 8. Example HR characteristics for 1400 and 2200 rpm.

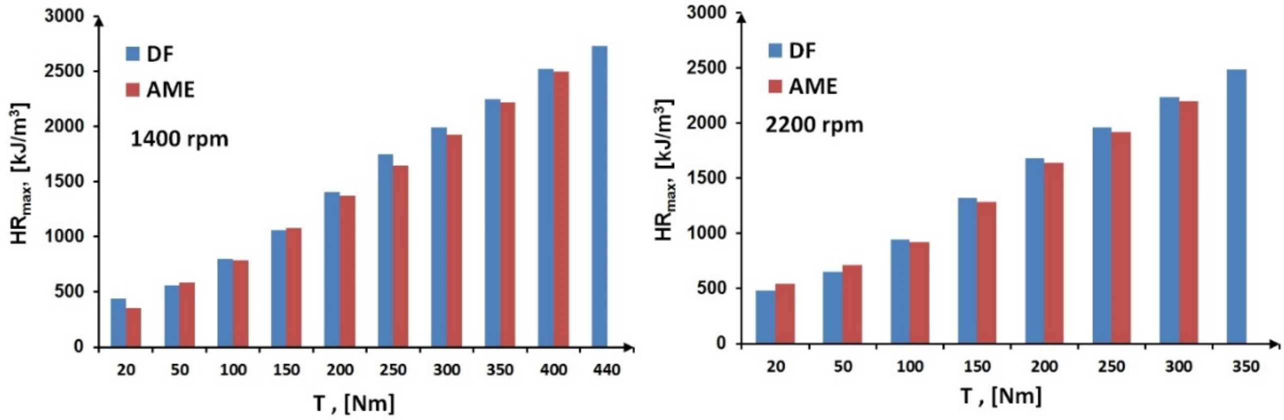

Figure 9. Maximum values HR_{max} for 1400 and 2200 rpm and feed DF and AME.

AVL software was used to determine the effect of the tested fuels on the rate of fuel dose burnout. Using this software, the values of CA angles at which 5, 10, 50, and 90% of the fuel dose burned out were determined. The method of determining these values is shown in Figure 12. The analysis of these data made it possible to determine the beginning of the combustion process, i.e., the 5% burnout, and the end of the combustion process, defined according to this methodology as the 90% burnout of the fuel dose.

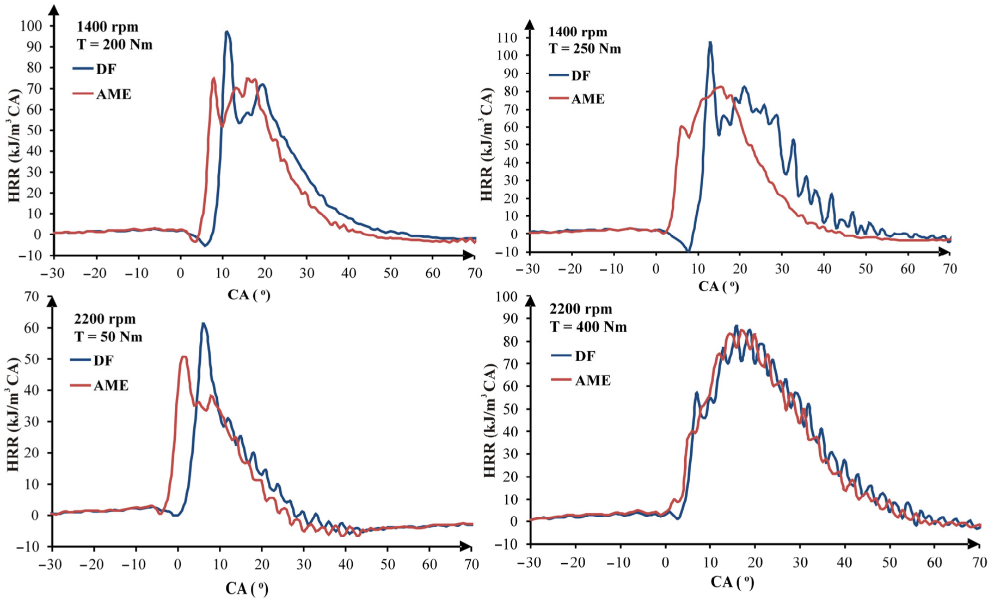

Figure 10. Example HRR characteristics for speeds 1400 and 2200 rpm.

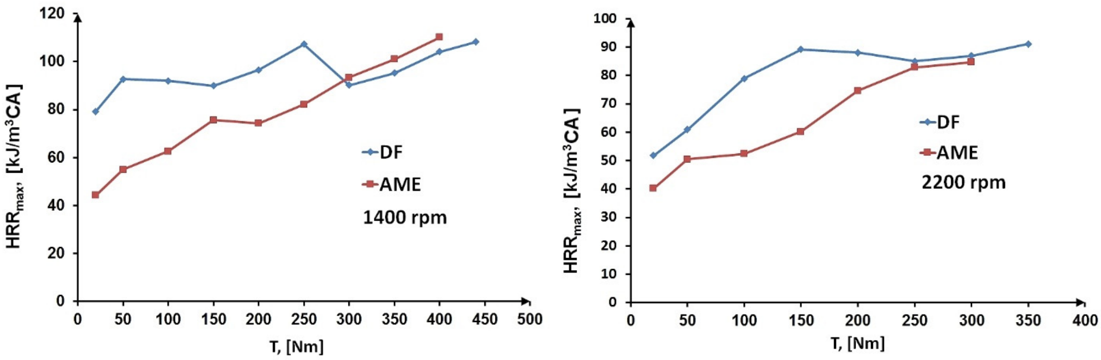

Figure 11. Maximum HRRmax at 1400 and 2200 rpm.

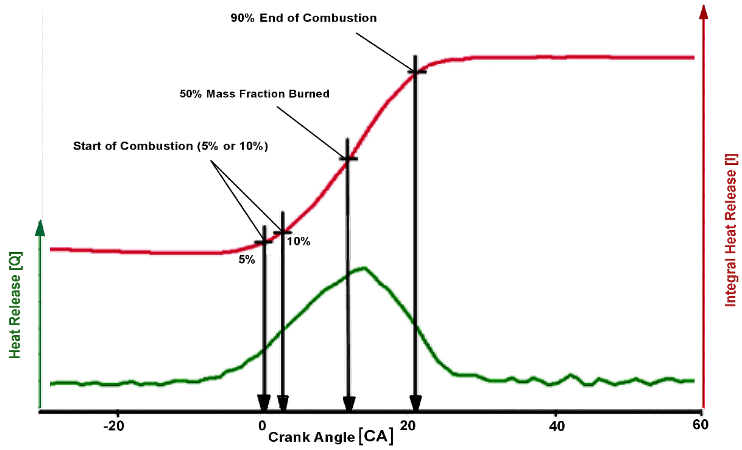

Figure 12. Methodology for determining the angles of engine crankshaft rotation at which the fuel dose was burned to the extent of 5, 10, 50, and 90% of the total fuel dose injected into the cylinder.

The angular values of CA and percent fuel dose firing are shown in Figures 13 and 14. The values obtained for 1400 rpm characteristics indicate faster fuel dose firing for AMEs compared to DF. This is related to the shorter auto-ignition delay for AMEs, but also due to the high oxygen content. These results are consistent with the work of [41,42]. The authors of these works also pointed out the earlier onset of combustion when fueling engines with biofuels. According to the methodology used, it is determined that the onset of combustion equates to burning 5 or 10% of the fuel dose. Analogous relationships are found for the speed of 2200 rpm. For most measurement points, the fastest fuel dose burnout was obtained for AMEs. These differences from DF are about 5° CA. For speeds of 2200 rpm and loads of 20 and 50 Nm, burning 5% of the fuel dose occurs faster for DF, about 3° CA. There is a similar relationship for the burnout of 50 and 90% of the fuel dose, where for a load of 20 Nm, faster burnout also occurred for DF. The results for both characteristics indicate that AMEs, like other biofuels, due to their properties and composition, burn faster compared to DF.

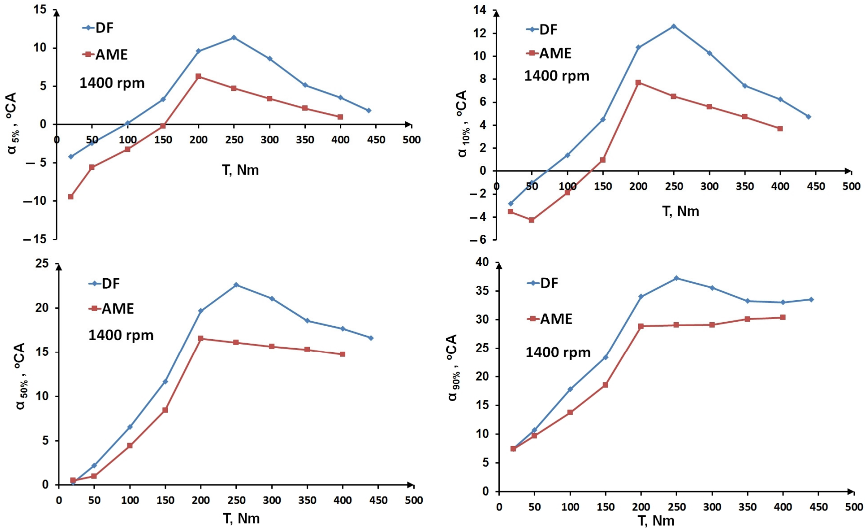

Figure 13. Angles of CA crankshaft revolutions at which the individual percentages of the fuel dose were burned off at characteristics of 1400 rpm.

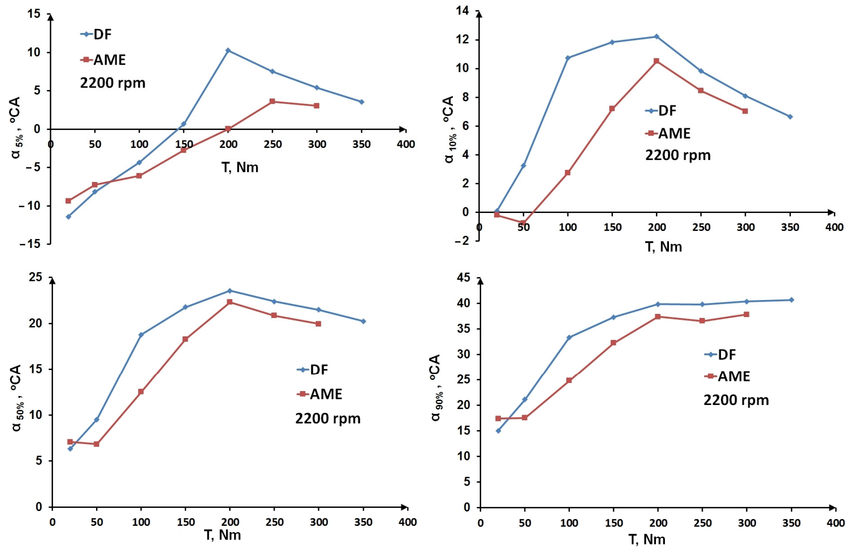

Figure 14. Angles of CA crankshaft rotation at which individual percentages of the fuel dose were burned off at 2200 rpm characteristics.

The results of the tests were subjected to statistical analysis by calculating the standard uncertainties of the arithmetic means, the basic measured and calculated indicators of engine operation, as well as the parameters of the combustion process, which are shown in Tables 5–8.

Table 5. Standard uncertainty of the arithmetic means of the measured and calculated indices and parameters of engine operation at n = 1400 rpm and feeding it with DF.

T (Nm)	Quantities Measured Directly									
	ΔT (Nm)	ΔP (kW)	ΔFC (kg/h)	Δpmax (MPa)	$\Delta\alpha_{pmax}$ (CA)	Δdp/dα (MPa/CA)	Δα 5% (CA)	Δα 10% (CA)	Δα 50% (CA)	Δα 90% (CA)
20	0.0076	0.0011	0.0014	0.0566	0.0405	0.0140	0.0214	0.0085	0.0127	0.0562
50	0.0169	0.0024	0.0079	0.0644	0.0598	0.0162	0.0172	0.0133	0.0183	0.0622
100	0.0113	0.0017	0.0115	0.0699	0.0500	0.0200	0.0117	0.0144	0.0314	0.0620
150	0.0170	0.0023	0.0396	0.0581	0.0768	0.0185	0.0171	0.0164	0.0342	0.0709
200	0.0126	0.0021	0.0093	0.0082	0.0157	0.0158	0.0208	0.0182	0.0300	0.0849
250	0.0136	0.0025	0.0036	0.0081	0.0151	0.0141	0.0140	0.0130	0.0244	0.0706
300	0.0131	0.0031	0.0075	0.0091	0.0154	0.0148	0.0134	0.0130	0.0216	0.0579
350	0.0170	0.0057	0.0277	0.0117	0.0194	0.0206	0.0111	0.0167	0.0227	0.0648
400	0.0181	0.0055	0.0136	0.0383	0.0961	0.0174	0.0110	0.0140	0.0242	0.0754
440	0.0076	0.0011	0.0125	0.0782	0.0880	0.0195	0.0149	0.0174	0.0279	0.0835

Table 6. Standard deviations of the arithmetic means of the measured and calculated indices and parameters of engine operation at n = 2200 rpm and feeding it with DF.

T (Nm)	Quantities Measured Directly									
	ΔT (Nm)	ΔP (kW)	ΔFC (kg/h)	Δpmax (MPa)	$\Delta\alpha_{pmax}$ (CA)	Δdp/dα (MPa/CA)	Δα 5% (CA)	Δα 10% (CA)	Δα 50% (CA)	Δα 90% (CA)
20	0.0528	0.0029	0.0014	0.0619	0.0620	0.0989	0.0586	0.0486	0.0236	0.0652
50	0.0111	0.0026	0.0023	0.0983	0.0768	0.0149	0.0698	0.0260	0.0385	0.0790
100	0.0122	0.0029	0.0030	0.0107	0.0295	0.0163	0.0804	0.0334	0.0463	0.0819
150	0.0095	0.0024	0.0118	0.0105	0.0188	0.0152	0.0101	0.0363	0.0439	0.0106
200	0.0116	0.0028	0.0117	0.0109	0.0203	0.0155	0.0391	0.0143	0.0360	0.0901
250	0.0131	0.0034	0.0050	0.0119	0.0292	0.0204	0.0300	0.0130	0.0317	0.0990
300	0.0135	0.0044	0.0360	0.0124	0.0201	0.0185	0.0185	0.0164	0.0308	0.0953
350	0.0124	0.0041	0.0254	0.0168	0.0148	0.0200	0.0148	0.0175	0.0297	0.0118

Table 7. Standard deviations of arithmetic means of measured and calculated indicators and parameters of engine operation at n = 1400 rpm and feeding it with AMEs.

T (Nm)	Quantities Measured Directly									
	ΔT (Nm)	ΔP (kW)	ΔFC (kg/h)	Δpmax (MPa)	$\Delta\alpha_{pmax}$ (CA)	Δdp/dα (MPa/CA)	Δα 5% (CA)	Δα 10% (CA)	Δα 50% (CA)	Δα 90% (CA)
20	0.0101	0.0015	0.0062	0.0461	0.0407	0.0133	0.0692	0.0112	0.0150	0.0346
50	0.0101	0.0016	0.0091	0.0716	0.0712	0.0960	0.0101	0.0122	0.0273	0.0462
100	0.0120	0.0019	0.0063	0.0850	0.0687	0.0202	0.0172	0.0148	0.0284	0.0519
150	0.0133	0.0022	0.0027	0.0746	0.0711	0.0271	0.0145	0.0125	0.0300	0.0606
200	0.0157	0.0042	0.0020	0.0085	0.0198	0.0187	0.0086	0.0093	0.0228	0.0591
250	0.0206	0.0053	0.0052	0.0123	0.0029	0.0256	0.0126	0.0109	0.0205	0.0577
300	0.0159	0.0065	0.0186	0.0434	0.0078	0.0158	0.0125	0.0123	0.0208	0.0548
350	0.0171	0.0054	0.0025	0.0590	0.0017	0.0977	0.0112	0.0163	0.0232	0.0698
400	0.0242	0.0091	0.0079	0.0664	0.0077	0.0217	0.0114	0.0139	0.0213	0.0806

Table 8. Standard deviations of arithmetic means of measured and calculated indicators and parameters of engine operation at n = 2200 rpm and feeding it with AMEs.

T (Nm)	Quantities Measured Directly									
	ΔT (Nm)	ΔP (kW)	ΔFC (kg/h)	Δpmax (MPa)	$\Delta\alpha_{pmax}$ (CA)	Δdp/dα (MPa/CA)	Δα 5% (CA)	Δα 10% (CA)	Δα 50% (CA)	Δα 90% (CA)
20	0.0097	0.0231	0.0318	0.0677	0.080	0.0614	0.0585	0.0220	0.0368	0.0673
50	0.0106	0.0253	0.0165	0.0769	0.084	0.0176	0.0681	0.0124	0.0330	0.0655
100	0.0115	0.0286	0.0363	0.0646	0.051	0.0249	0.0498	0.0210	0.0385	0.0631
150	0.0190	0.0459	0.0410	0.0160	0.039	0.0201	0.0579	0.0246	0.0424	0.0932
200	0.0119	0.0313	0.0343	0.0115	0.021	0.0169	0.0390	0.0147	0.0266	0.0819
250	0.0138	0.0351	0.0251	0.0130	0.027	0.0193	0.0867	0.0142	0.0289	0.0922
300	0.0154	0.0664	0.0684	0.0133	0.060	0.0185	0.0378	0.0163	0.0249	0.0963

4. Conclusions

The research presented in this article, along with its results and analysis, made it possible to determine the effect on the combustion process of feeding a Perkins 1104D-E44TA compression ignition engine with animal waste ethyl esters (AMEs), compared to feeding it with diesel fuel (DF). The analysis of the test results showed that feeding the engine with AMEs results in a decrease in the maximum torque at 1400 rpm from 440 to 400 Nm. At 2200 rpm, the torque dropped from 350 Nm for DF to 300 Nm for AME. The decrease in torque when feeding the engine with AMEs may be due to increased viscosity negatively affecting the course of combustible mixture formation and combustion, which is also confirmed by studies [55–57,67–74] and the lower heating value of this fuel. The decrease in torque when burning AMEs can significantly limit its use as a fuel for heavily loaded engines. In addition, feeding the engine with AMEs, increases fuel consumption by a maximum of 15% compared to DF. Only at certain measurement points is it very close to DF.

When feeding the engine with AMEs at 1400 rpm in the low and high load ranges, an approximately 10% higher p_{max} was obtained compared to DF; this is strongly dependent on engine load. At a characteristic of 2200 rpm at low loads, the relationship is similar, while as the load increases, the p_{max} values for both fuels are similar. Moreover, for AMEs at 1400 rpm for low and medium loads up to T = 100 Nm, the maximum pressure p_{max} occurred slightly earlier compared to DF by about 2° CA. For higher loads, the relationship is reversed.

For 2200 rpm characteristics, the relationships are similar to those for 1400 rpm, but the differences in α_{pmax} values are greater at lower loads. For loads from 20 to 50 Nm when feeding the AME engine, the maximum combustion pressure occurred earlier compared to DF by about 10° CA. For other loads, the relationship is reversed. The analysis of rising pressure during the combustion process showed that feeding the engine with AMEs for most loads causes much higher maximum pressure rises during the combustion process compared to those obtained by feeding it DF. These values are higher for AMEs by up to 40%. This is due to the earlier start of the combustion process and the higher oxygen content of AMEs compared to DF. Larger pressure increases during the combustion process can negatively affect the durability of the engine's crank–piston components. HR_{max} characteristics drawn up from the pressure profile showed that they are slightly higher at low loads when feeding the engine with AMEs compared to those obtained with DF. For most of the measurement points for the two load characteristics, the HR_{max} values are larger when feeding the engine DF by a maximum of about 20%, which is due to the lower calorific value of AMEs compared to DF. In the case of heat release rate, these values are higher for DF compared to AMEs by a maximum of about 44%.

The analysis of the values of the maximum heat release rate HRR_{max} at 1400 rpm as well as 2200 rpm revealed that feeding the engine with AME fuel results in lower heat release rate values. This sis particularly pronounced for small and medium engine loads in the range from 20 to 200–250 Nm. The values are higher for DF by up to 44%, with larger differences for 1400 rpm. Only for a few loads were the values larger for AMEs, by about 7%. The smaller HRR_{max} value for AMEs are due to the lower heating value of this fuel as well as its density and viscosity. The analysis of the angular values of the burnout of individual fuel dose percentages showed that for most loads, feeding the engine with AMEs results in a faster burnout of the fuel dose compared to DF, from 3° to 6° CA for 1400 rpm. For the 2200 rpm characteristic, the biggest differences occur for the burnout of 10% of the fuel dose and amount to a maximum of 10° CA. This is due to the shorter auto-ignition delay for biofuels, but also high oxygen content.

Author Contributions: P.Ł.: data curation, writing—original draft, writing—review and editing, and visualization. D.K.: data curation, visualization, and writing—original draft. G.W.: writing—original draft and writing—review and editing. All authors have read and agreed to the published version of the manuscript.

Funding: This research was funded by the Faculty of Mechatronics and Mechanical Engineering, Kielce University of Technology, and the Faculty of Production Engineering and Power Technologies, University of Agriculture in Krakow.

Institutional Review Board Statement: Not applicable.

Informed Consent Statement: Not applicable.

Data Availability Statement: The data presented in this study are available from the corresponding author on reasonable request.

Conflicts of Interest: The authors declare no conflict of interest.

Nomenclature

AME	animal methyl esters
BTE	brake thermal efficiency
BSFC	brake-specific fuel consumption
HVO	hydrotreated vegetable oil
RME	rapeseed Oil Methyl Esters
CA	crank angle, deg
DF	diesel fuel
dp/dα	degree of pressure build-up, MPa/CA
HR	amount of heat release, kJ/m^3
HRR	heat release rates, kJ/m^3 CA
HR_{max}	maximum heat release, kJ/m^3
HRR_{max}	maximum heat release rates, kJ/m^3 CA
p	cylinder pressure, MPa
p_{max}	maximum combustion pressure, MPa
T	torque, Nm
$\alpha_{5\%}$	burnout angle of 5% fuel dose, CA
$\alpha_{10\%}$	burnout angle of 10% fuel dose, CA
$\alpha_{50\%}$	burnout angle of 50% fuel dose, CA
$\alpha_{90\%}$	burnout angle of 90% fuel dose, CA
α_{pmax}	angle of onset of maximum cylinder pressure, CA

References

1. Naik, S.N.; Goud, V.V.; Rout, P.K.; Dalai, A.K. Production of first and second generation biofuels: A comprehensive review. *Renew. Sustain. Energy Rev.* **2010**, *14*, 578–597. [CrossRef]
2. Bhuiya, M.M.K.; Rasul, M.G.; Khan, M.M.K.; Ashwath, N.; Azad, A.K. Prospects of 2nd generation biodiesel as a sustainable fuel—Part: 1 selection of feedstocks, oil extraction techniques and conversion technologies. *Renew. Sustain. Energy Rev.* **2016**, *55*, 1109–1128. [CrossRef]
3. Yaşar, F. Comparison of fuel properties of biodiesel fuels produced from different oils $_T$ to determine the most suitable feedstock type. *Fuel* **2020**, *264*, 116817. [CrossRef]
4. Klimiuk, E.; Pawłowska, M.; Pokój, T. *Biofuels. Technologies for Sustainable Development*; Polish Scientific Publishers PWN: Warsaw, Poland, 2012.
5. Tayari, S.; Abedi, R.; Rahi, A. Comparative assessment of engine performance and emissions fueled with three different biodiesel generations. *Renew. Energy* **2020**, *147*, 1058–1069. [CrossRef]
6. Zhong, W.; Xuan, T.; He, Z.; Wang, Q.; Li, D.; Zhang, X.; Yin, H.Y. Experimental study of combustion and emission characteristics of diesel engine with diesel/second-generation biodiesel blending fuels. *Energy Convers. Manag.* **2016**, *121*, 241–250. [CrossRef]
7. Singh, D.; Sharma, D.; Soni, S.L.; Sharma, S.; Kumari, D. Chemical compositions, properties, and standards for different generation biodiesels: A review. *Fuel* **2019**, *253*, 60–71. [CrossRef]
8. Saravanan, A.; Murugan, M.; Sreenivasa, R.M.; Parida, S. Performance and emission characteristics of variable compression ratio CI engine fueled with dual biodiesel blends of Rapeseed and Mahua. *Fuel* **2020**, *263*, 116751. [CrossRef]
9. Sakthivel, R.; Ramesh, K.; Purnachandran, R.; Shameer, P.M. A review on the properties, performance and emission aspects of the third generation biodiesels. *Renew. Sustain. Energy Rev.* **2018**, *82*, 2970–2992. [CrossRef]
10. Saladini, F.; Patrizi, N.; Pulselli, F.M.; Marchettini, N.; Bastianoni, S. Guidelines for energy evaluation of first, second and third generation biofuels. *Renew. Sustain. Energy Rev.* **2016**, *66*, 221–227. [CrossRef]
11. Buyukkaya, E. Effects of biodiesel on a DI diesel engine performance, emission and combustion characteristics. *Fuel* **2010**, *89*, 3099–3105. [CrossRef]

12. Caresana, F.; Bietresato, M.; Renzi, M. Injection and Combustion Analysis of Pure Rapeseed Oil Methyl Ester (RME) in a Pump-Line-Nozzle Fuel Injection System. *Energies* **2021**, *14*, 7535. [CrossRef]
13. Korakianitis, T.; Namasivayam, A.M.; Crookes, R.J. Diesel and rapeseed methyl ester (RME) pilot fuels for hydrogen and natural gas dual-fuel combustion in compression–ignition engines. *Fuel* **2011**, *90*, 2384–2395. [CrossRef]
14. Özener, O.; Yuksek, L.; Ergenc, A.T.; Ozkan, M. Effects of soybean biodiesel on a DI diesel engine performance, emission and combustion characteristics. *Fuel* **2014**, *115*, 875–883. [CrossRef]
15. Kassem, Y.; Çamur, H. Effects of storage under different conditions on the fuel properties of biodiesel admixtures derived from waste frying and canola oils. *Biomass Convers. Biorefinery* **2018**, *8*, 825–845. [CrossRef]
16. Puhan, S.; Jegan, R.; Balasubbramanian, K.; Nagarajan, G. Effect of injection pressure on performance, emission and combustion characteristics of high linolenic linseed oil methyl ester ina DI diesel engine. *Renew. Energy* **2009**, *34*, 1227–1233. [CrossRef]
17. Ranucci, C.R.; Alves, H.J.; Monteiro, M.R.; Kugelmeier, C.L.; Bariccatti, R.A.; de Oliveira, C.R.; da Silva, E.A. Potential alternative aviation fuel from jatropha (*Jatropha curcas* L.), babassu (*Orbignya phalerata*) and palm kernel (*Elaeis guineensis)* as blends with Jet-A1 kerosene. *J. Clean. Prod.* **2018**, *185*, 860–869. [CrossRef]
18. Dyrektywa 2003/30/WE Parlamentu Europejskiego i Rady z dnia 8 maja 2003 r. w Sprawie Wspierania Użycia w Transporcie Biopaliw Lub Innych Paliw Odnawialnych. Available online: https://eur-lex.europa.eu/legal-content/PL/ALL/?uri=CELEX:32003L0030 (accessed on 13 July 2022). (In Polish).
19. Dyrektywa Parlamentu Europejskiego i Rady 2009/28/WE z dnia 23 Kwietnia 2009 r. w Sprawie Promowania Stosowania Energii ze Źródeł Odnawialnych Zmieniająca i w Następstwie Uchylająca Dyrektywy 2001/77/WE Oraz 2003/30/WE. Available online: https://eur-lex.europa.eu/legal-content/PL/ALL/?uri=CELEX:32009L0028 (accessed on 13 July 2022). (In Polish).
20. Boutesteijn, C.; Drabik, D.; Venus, T.J. The interaction between EU biofuel policy and first- and second-generation biodiesel production. *Ind. Crops Prod.* **2017**, *106*, 124–129. [CrossRef]
21. Biernat, K. Perspektywy rozwoju technologii biopaliwowych w świecie do 2050 roku. *Chemik* **2012**, *11*, 1178–1189. (In Polish)
22. Labeckas, G.; Slavinskas, S. Performance of direct-injection off-road diesel engine on rapeseed oil. *Renew. Energy* **2006**, *31*, 849–863. [CrossRef]
23. Karabektas, M.; Ergen, G.; Hosoz, M. Effects of the blends containing low ratios of alternative fuels on the performance and emission characteristics of a diesel engine. *Fuel* **2013**, *112*, 537–541. [CrossRef]
24. Sakthivel, G.; Sivaraja, C.M.; Ikua, B.W. Prediction OF CI engine performance, emission and combustion parameters using fish oil as a biodiesel by fuzzy-GA. *Energy* **2019**, *166*, 287–306. [CrossRef]
25. Banković-Ilić, I.B.; Stojković, I.J.; Stamenković, O.S.; Veljkovic, V.B.; Hung, Y.-T. Waste animal fats as feedstocks for biodiesel production. *Renew. Sustain. Energy Rev.* **2014**, *32*, 238–254. [CrossRef]
26. Adewale, P.; Dumont, M.-J.; Ngadi, M. Recent trends of biodiesel production from animal fat wastes and associated production techniques. *Renew. Sustain. Energy Rev.* **2015**, *45*, 574–588. [CrossRef]
27. Zarska, M.; Bartoszek, K.; Dzida, M. High pressure physicochemical properties of biodiesel components derived from coconut oil or babassu oil. *Fuel* **2014**, *125*, 144–151. [CrossRef]
28. Kumar, N.; Chauhan, S.R. Performance and emission characteristics of biodiesel from different origins. A review. *Renew. Sustain. Energy Rev.* **2013**, *21*, 633–658. [CrossRef]
29. Estevez, R.; Aguado-Deblas, L.; López-Tenllado, F.J.; Luna, C.; Calero, J.; Romero, A.A.; Bautista, M.F.; Luna, D. Biodiesel Is Dead: Long Life to Advanced Biofuels—A Comprehensive Critical Review. *Energies* **2022**, *15*, 3173. [CrossRef]
30. Ramos, M.; Dias, A.P.S.; Puna, J.F.; Gomes, J.; Bordado, J.C. Biodiesel production processes and sustainable raw materials. *Energies* **2019**, *12*, 4408. [CrossRef]
31. Mani, M.; Nagarajan, G.; Sampath, S. Characterisation and effect of using waste plastic oil and diesel fuel blends in compression ignition engine. *Energy* **2011**, *36*, 212–219. [CrossRef]
32. Chen, J.; Li, J.; Dong, W.; Zhang, X.; Tyagi, R.D.; Drogui, P.; Surampalli, R.Y. The potential of microalgae in biodiesel production. *Renew. Sustain. Energy Rev.* **2018**, *90*, 336–346. [CrossRef]
33. Hariram, V.; Kumar, G.M. Combustion analysis of algal oil methyl ester in a direct injection compression ignition engine. *J. Eng. Sci. Technol.* **2013**, *8*, 77–92.
34. Cunha, A.; Feddern, V.; De Prá, M.C.; Higarashi, M.M.; de Abreu, P.G.; Coldebella, A. Synthesis and characterization of ethylic biodiesel from animal fat wastes. *Fuel* **2013**, *105*, 228–234. [CrossRef]
35. Alptekin, E.; Canakci, M.; Sanli, H. Biodiesel production from vegetable oil and waste animal fats in a pilot plant. *Waste Manag.* **2014**, *34*, 2146–2154. [CrossRef] [PubMed]
36. Encinar, J.M.; Sánchez, N.; Martínez, G.; García, L. Study of biodiesel production from animal fats with high free fatty acid content. *Bioresour. Technol.* **2011**, *102*, 10907–10914. [CrossRef]
37. Teixeira, M.A.; da Graça Carvalho, M. Regulatory mechanism for biomass renewable energy in Brazil, a case study of the Brazilian Babassu oil extraction industry. *Energy* **2007**, *32*, 999–1005. [CrossRef]
38. Orliński, P.; Sikora, M.; Bednarski, M.; Gis, M. The Influence of Powering a Compression Ignition Engine with HVO Fuel on the Specific Emissions of Selected Toxic Exhaust Components. *Appl. Sci.* **2024**, *14*, 5893. [CrossRef]
39. Gharehghani, A.; Mirsalim, M.; Hosseini, R. Effects of waste fish oil biodiesel on diesel engine combustion characteristics and emission. *Renew. Energy* **2017**, *101*, 930–936. [CrossRef]

40. Badday, A.S.; Abdullah, A.Z.; Lee, K.-T. Optimization of biodiesel production process from Jatropha oil using supported heteropolyacid catalyst and assisted by ultrasonic energy. *Renew. Energy* **2013**, *50*, 427–432. [CrossRef]
41. Varuvel, G.; Mrad, N.; Tazerout, M.; Aloui, F. Experimental analysis of biofuel as an alternative fuel for diesel engines. *Appl. Energy* **2012**, *94*, 224–231. [CrossRef]
42. Alptekin, E.; Canakci, M.; Ozsezen, A.N.; Turkcan, A.; Sanli, H. Using waste animal fat based biodiesels–bioethanol–diesel fuel blends in a DI diesel engine. *Fuel* **2015**, *157*, 245–254. [CrossRef]
43. Łabecki, L.; Cairns, A.; Xia, J.; Megaritis, A.; Zhao, H.; Ganippa, L. Combustion and emission of rapeseed oil blends in diesel engine. *Appl. Energy* **2012**, *95*, 139–146. [CrossRef]
44. Sathish, T.; Agbulut, Ü.; Kumari, V.; Rathinasabapathi, G.; Karthikumar, K.; Jyothi, N.R.; Kandavalli, S.R.; Muni, T.V.; Saravanan, R. Energy recovery from waste animal fats and detailed testing on combustion, performance, and emission analysis of IC engine fueled with their blends enriched with metal oxide nanoparticles. *Energy* **2023**, *284*, 129287. [CrossRef]
45. Gad, M.S.; Uysal, C.; El-Shafay, A.S.; Ağbulut, Ü. Exergetic and exergoeconomic assessments of a diesel engine fuelled with waste chicken fat biodiesel-diesel blends. *Energy* **2024**, *293*, 130676. [CrossRef]
46. Heywood, J.B. *Internal Combustion Engines Fundamentals*; McGraw-Hill: New York, NY, USA, 1988.
47. Ambrozik, A. *Analiza Cykli Pracy Czterosuwowych Silników Spalinowych*; Wydawnictwo Politechniki Świętokrzyskiej w Kielcach: Kielce, Poland, 2010. (In Polish)
48. Kurczyński, D.; Łagowski, P. Performance indices of a common rail-system CI engine powered by diesel oil and biofuel blends. *J. Energy Inst.* **2019**, *92*, 1897–1913. [CrossRef]
49. Orliński, P.; Laskowski, P.; Zimakowska-Laskowska, M.; Mazuruk, P. Assessment of the Impact of the Addition of Biomethanol to Diesel Fuel on the Coking Process of Diesel Engine Injectors. *Energies* **2022**, *15*, 688. [CrossRef]
50. Kamela, W.; Wojs, M.K.; Orliński, P. Calculation Method for Assessing the Storage Capacity of Nitrogen Compounds in LNT Reactors. *Energies* **2022**, *15*, 7819. [CrossRef]
51. Laskowska, M.; Laskowski, P.; Wojs, M.K.; Orliński, P. Prediction of Pollutant Emissions in Various Cases in Road Transport. *Appl. Sci.* **2022**, *12*, 11975. [CrossRef]
52. AVL. AVL-Development, Testing & Simulation of Powertrain Systems. Available online: https://www.avl.com/?avlregion=GLOBAL&groupId=10138&lang=en_US (accessed on 13 July 2022).
53. *PN-EN 590+A1:2017-06*; Paliwa do Pojazdów Samochodowych. Oleje Napędowe. Wymagania i Metody Badań. Polski Komitet Normalizacyjny: Warsaw, Poland, 2017. (In Polish)
54. Milojević, S.; Glišović, J.; Savić, S.; Bošković, G.; Bukvić, M.; Stojanović, B. Particulate Matter Emission and Air Pollution Reduction by Applying Variable Systems in Tribologically Optimized Diesel Engines for Vehicles in Road Traffic. *Atmosphere* **2024**, *15*, 184. [CrossRef]
55. Kurczyński, D.; Wcisło, G.; Łagowski, P. Experimental Study of Fuel Consumption and Exhaust Gas Composition of a Diesel Engine Powered by Biodiesel from Waste of Animal Origin. *Energies* **2021**, *14*, 3472. [CrossRef]
56. Qi, D.; Bae, C.; Feng, Y.; Jia, C.; Bian, Y. Combustion and emission characteristics of a direct injection compression ignition engine using rapeseed oil based microemulsions. *Fuel* **2013**, *107*, 570–577. [CrossRef]
57. Kuszewski, H. Experimental investigation of the autoignition properties of ethanol–biodiesel fuel blends. *Fuel* **2019**, *235*, 1301–1308. [CrossRef]
58. *PN-C-04375-3:2013-07*; Badanie Paliw Stałych i Ciekłych. Oznaczanie Ciepła Spalania w Bombie Kalorymetrycznej i Obliczanie Wartości Opałowej. Część 3: Metoda z Zastosowaniem Kalorymetru z Płaszczem Adiabatycznym. Polski Komitet Normalizacyjny: Warsaw, Poland, 2013. (In Polish)
59. *PN-EN ISO 2719:2016-08*; Oznaczanie Temperatury Zapłonu. Metoda Zamkniętego Tygla Pensky'ego-Martensa. Polski Komitet Normalizacyjny: Warsaw, Poland, 2018. (In Polish)
60. *PN-EN ISO 3104:2004*; Oznaczanie Lepkości Kinematycznej i Obliczanie Lepkości Dynamicznej Paliw i Biopaliw. Polski Komitet Normalizacyjny: Warsaw, Poland, 2004. (In Polish)
61. *PN-EN ISO 12185:2002*; Ropa Naftowa i Przetwory Naftowe. Oznaczanie Gęstości. Metoda Oscylacyjna z U-rurką. Polski Komitet Normalizacyjny: Warsaw, Poland, 2002. (In Polish)
62. *PN-EN ISO 5165:2003*; Przetwory Naftowe. Oznaczanie Właściwości Zapłonowych Olejów Napędowych. Metoda Silnikowa Oznaczania Liczby Cetanowej. Polski Komitet Normalizacyjny: Warsaw, Poland, 2003. (In Polish)
63. *PN-EN ISO 12937:2005*; Przetwory Naftowe. Oznaczanie Wody—Miareczkowanie Kulometryczne Metodą Karla Fischera. Polski Komitet Normalizacyjny: Warsaw, Poland, 2005. (In Polish)
64. *EN 116:2015*; Diesel and Domestic Heating Fuels-Determination of Cold Filter Plugging Point-Stepwise Cooling Bath Method. Polski Komitet Normalizacyjny: Warsaw, Poland, 2015.
65. *PN-EN ISO 12156-1:2018-12*; Oleje Napędowe-Ocena Smarności z Zastosowaniem Aparatu o Ruchu Posuwisto-Zwrotnym Wysokiej Częstotliwości (HFRR). Część 1: Metoda Badania. Polski Komitet Normalizacyjny: Warsaw, Poland, 2018. (In Polish)
66. *PN-EN 14103:2012*; Produkty Przetwarzania Olejów i Tłuszczów. Estry Metylowe Kwasów Tłuszczowych (FAME). Oznaczanie Zawartości Estrów i Estru Metylowego Kwasu Linolenowego. Polski Komitet Normalizacyjny: Warsaw, Poland, 2012. (In Polish)
67. Żółty, M.; Krasodomski, W. Stabilność oksydacyjna estrów metylowych kwasów tłuszczowych stanowiących samoistne paliwo lub biokomponent olejów napędowych. *Nafta-Gaz* **2017**, *5*, 399–405. (In Polish) [CrossRef]

68. Wcisło, G. *Analiza Wpływu Odmian Rzepaku na Właściwości Biopaliw RME i Parametry Pracy Silnika o Zapłonie Samoczynnym*; Wydawnictwo FALL: Kraków, Poland, 2013. (In Polish)
69. Milojević, S.; Savić, S.; Marić, D.; Stopka, O.; Krstić, B.; Stojanović, B. Correlation between Emission and Combustion Characteristics with the Compression Ratio and Fuel Injection Timing in Tribologically Optimized Diesel Engine. *Teh. Vjesn.* **2022**, *29*, 1210–1219. [CrossRef]
70. Gajević, S.; Marković, A.; Milojević, S.; Ašonja, A.; Ivanović, L.; Stojanović, B. Multi-Objective Optimization of Tribological Characteristics for Aluminum Composite Using Taguchi Grey and TOPSIS Approaches. *Lubricants* **2024**, *12*, 171. [CrossRef]
71. Lee, K.; Cho, H. Comparative Analysis of Performance and Emission Characteristics of Biodiesels from Animal Fats and Vegetable Oils as Fuel for Common Rail Engines. *Energies* **2024**, *17*, 1711. [CrossRef]
72. Pramudito, Y.; Wirahadi, D.; Faturrahman, N.A.; Supriadi, F.; Bethari, S.A.; Rulianto, D.; Widodo, S.; Respatiningsih, C.Y.; Aisyah, L.; Wibowo, C.S.; et al. Comparison performance ci engine of using high-speed diesel fuel-biodiesel blend (b30) and (b40) on diesel engine dyno test. *IOP Conf. Ser. Earth Environ. Sci.* **2022**, *1034*, 012058. [CrossRef]
73. Czarnocka, J.; Malinowski, A.; Sitnik, L. Assessment of physicochemical properties ternary biofuels to power diesel engines. *Arch. Motoryz.* **2011**, *4*, 39–44. (In Polish) [CrossRef]
74. Dhande, D.Y.; Navale, S.J. The experimental investigations on the performance and emissions of compression ignition engine fuelled with lower blends of neem-based biodiesel Archives of Automotive Engineering. *Arch. Motoryz.* **2024**, *103*, 57. [CrossRef]